

# Modeling the ion channel structure of cecropin

Stewart R. Durell, Gopalan Raghunathan, and H. Robert Guy

Laboratory of Mathematical Biology, National Cancer Institute, National Institutes of Health, Bethesda, Maryland 20892 USA

**ABSTRACT** Atomic-scale computer models were developed for how cecropin peptides may assemble in membranes to form two types of ion channels. The models are based on experimental data and physiochemical principles. Initially, cecropin peptides, in a helix-bend-helix motif, were arranged as antiparallel dimers to position conserved residues of adjacent monomers in contact. The dimers were postulated to bind to the membrane with the NH<sub>2</sub>-terminal helices sunken into the head-group layer and the COOH-terminal helices spanning the hydrophobic core. This causes a thinning of the top lipid layer of the membrane. A collection of the membrane bound dimers were then used to form the type I channel structure, with the pore formed by the transmembrane COOH-terminal helices. Type I channels were then assembled into a hexagonal lattice to explain the large number of peptides that bind to the bacterium. A concerted conformational change of a type I channel leads to the larger type II channel, in which the pore is formed by the NH<sub>2</sub>-terminal helices. By having the dimers move together, the NH<sub>2</sub>-terminal helices are inserted into the hydrophobic core without having to desolvate the charged residues. It is also shown how this could bring lipid head-groups into the pore lining.

## INTRODUCTION

Cecropins are antimicrobial peptides identified as part of the immune response of three silkworm species (*Hyalophora cecropia*, *Antheraea pernyi*, and *Bombyx mori*) (1–5). There are three types of cecropin, A, B, and D, with 35–38 residues (see Fig. 1). In addition to killing bacteria, the cecropins have been shown to permeabilize liposomes and to form anion selective channels in lipid bilayers (6, 7). Other naturally occurring peptides that have been shown to form ion channels include alamethicin (8), magainin (9),  $\delta$ -lysin (10), defensin (11), and pardaxin (12).

The secondary structure of cecropin was predicted to have a helix-bend-helix motif from sequence analysis and circular dichroism measurements (13, 14). This was confirmed for cecropin A in reduced polarity solvent by two-dimensional nuclear magnetic resonance (NMR) analysis (15). The NH<sub>2</sub>-terminal helix has a net positive formal charge (+6e in cecropin A) and is amphipathic, whereas the COOH-terminal helix is less charged (+1e in cecropin A and D and neutral in cecropin B) and is more hydrophobic. The hinge between the helices is formed by the Gly 23 and Pro 24 residues, which are conserved in all of the cecropin sequences. Christensen et al. (7) and Fink et al. (16) have proposed models for how cecropin would initially bind to the membrane and form ion channels. In summary, the positively charged NH<sub>2</sub>-terminal helices bind to negatively charged head-groups on the membrane surface and the hydrophobic COOH-terminal helices insert into the membrane core. Then, the application of a positive potential, on the same side of the membrane as the peptides, pushes the positively charged NH<sub>2</sub>-terminal helices into the membrane. The channel would be formed by the association of multiple transmembrane NH<sub>2</sub>-terminal helices, such that the hydrophilic residues form the aqueous pore and the

hydrophobic residues are in contact with the aliphatic phase of the membrane.

Building on these ideas, we have developed atomic-scale computer models of cecropin ion channel structures. The models are designated either type I or type II to indicate whether the pores are formed by the COOH- or NH<sub>2</sub>-terminal helices, respectively. In addition to standard prediction methods and theoretical principles, the models were developed from the following experimental findings:

(a) There is a high degree of sequence conservation in the NH<sub>2</sub>-terminal and hinge regions of the cecropins and among the homologous bactericidin and sarcotoxin sequences, whereas the COOH-terminal region is less well conserved (17).

(b) The ion channels are voltage dependent, and the hinge region is required for this behavior. The chimeric cecropin AD peptide (which has the first 11 residues from *H.c.* cecropin A and the final 26 residues from *H.c.* cecropin D) displays a symmetric current-voltage curve. In addition, the cecropin AD and B peptides form channels with two distinct conduction states. The ability of cecropin to form channels is considerably greater for negatively charged membranes than for positively charged ones (7).

(c) The ability of cecropin to disrupt liposomes and form ion channels correlates with the antibacterial activity. A positively charged NH<sub>2</sub>-terminal helix, a hydrophobic COOH-terminal helix, and the intervening hinge are important structural elements for activity. Substitution of the conserved Trp 2 to a nonaromatic residue greatly decreases activity. A large number of cecropin molecules must be bound to the bacterial membrane to cause lysis. The calculated membrane surface area per bound cecropin A peptide at the 50% lethal dose concentration (LD50) is 660 Å<sup>2</sup>/peptide for *Escherichia coli* and 400 Å<sup>2</sup>/peptide for *Bacillus megaterium* (6, 7, 16, 18, 19).

Address correspondence to H. Robert Guy.

## METHODS

The guiding principles in designing the multimeric peptide models were to maximize the number of contacts between conserved residues, maximize the number of salt-bridges and hydrogen bonds, avoid internal cavities, and to position the hydrophobic and hydrophilic residues in the correct polarity environments.

## Protein structure

The first step was to fold the peptide monomer into the helix-bend-helix motif determined for the solution conformation of cecropin A by NMR (15). Deviating from the NMR results, the NH<sub>2</sub>-terminal helix was formed between residues 4 and 22, rather than between 5 and 21. This was to account for the presence of Asn 3 and Pro 4 in cecropin D, which are the most common residues to form the NH<sub>2</sub>-terminal cap and start of an  $\alpha$ -helix (20). Likewise, all of the cecropins have the Ala 22 residue, which has a high propensity for  $\alpha$ -helix conformation (20). The COOH-terminal helix was formed from the conserved Pro 24 residue to the end of the peptide, as indicated by the NMR results. The helices were formed by applying the standard  $\alpha$ -helix phi, psi, and omega angles to the peptide backbone. The side-chains were given the conformations that occur most commonly in  $\alpha$ -helices.

The next steps were to form an antiparallel dimer from two peptides and then use multiple dimers to construct channels. An iterative procedure of "manual" adjustment and automated energy minimization of side-chain and backbone conformations was used to eliminate atomic overlap and unfavorable charge and polarity interactions. This also served to maximize van der Waals contact, remove internal cavities and gaps between adjacent helices, and increase the number of salt-bridges and hydrogen bonds. To reduce the computational time, large structures were modeled from a relatively small asymmetric unit and energy minimized with symmetric images. It should be noted that the use of symmetry provided a constraint on the number of possible multimeric structures.

## Energy minimization

Energy minimization was carried out with the CHARMM molecular mechanics program (Molecular Simulations, Waltham, MA) (21). The polar hydrogen/extended atom topology and PARM30 parameter sets supplied by Molecular Simulations were used. Except for a distance-dependent dielectric constant, no attempt was made to include the effects of the solvent in the potential energy calculations. Likewise, except for explicitly placed phosphatidylserine and phosphatidylethanolamine molecules, no attempt was made to include the effects of the membrane in the calculations. To compensate for the lack of hydrophobic forces in the energy function, special attention was given to positioning the side-chains in the correct polarity environments. For example, hydrophobic residues were made to contact other hydrophobic residues or lipid alkyl chains, and hydrophilic residues were made to contact other hydrophilic residues, the solvent, or lipid head-groups. The only goal of the energy minimization procedure was to optimize packing; no attempt was made to judge the correctness of a structure from its relative potential energy.

## RESULTS

### Sequence analysis

Fig. 1 shows the alignment of the cecropin A, B, and D sequences with the related bactericidin (from tobacco hornworm) (22) and sarcotoxin (from flesh fly) (23) peptides. The sequences are very similar with many of the substitutions being conservative. Four residues in the NH<sub>2</sub>-terminal region are identical among all of the se-

Cecropins	1	5	10	15	20	25	30	35
H.c. A	KWKl <b>FKk</b> IEKvGQnIRDGIIk <b>AGPA</b> VavVGqAtqIaK-nh <sub>2</sub>							
H.c. B	KWKv <b>FKk</b> IEKvGRnIRNGIVk <b>AGPA</b> IavLGeAkaLg-nh <sub>2</sub>							
A.p. B	KWKi <b>FKk</b> IEKvGRnIRNGIIk <b>AGPA</b> VavLGeAkaLs-nh <sub>2</sub>							
B.m. B	RWKi <b>FKk</b> IEKvGRnIRDGIVk <b>AGPA</b> IevLGSaKaI-nh <sub>2</sub>							
H.c. D	-WNp <b>FKk</b> LEKvGQRVRDAVIS <b>AGPA</b> VatVAqAtaLaK-nh <sub>2</sub>							
A.p. D	-WNp <b>FKk</b> LERaGQRVRDAIIS <b>AGPA</b> VatVAqAtaLaK-nh <sub>2</sub>							
<b>Bactericidins</b>								
M.s. 2	-WNp <b>FKk</b> LERaGQRVRDAVIS <b>AaPA</b> VatVGqAaaIaR-nh <sub>2</sub>							
M.s. 3	-WNp <b>FKk</b> LERaGQRVRDAIIS <b>AGPA</b> VatVGqAaaIa-nh <sub>2</sub>							
M.s. 4	-WNp <b>FKk</b> LERaGQRVRDAIIS <b>AaPA</b> VatVGqAaaIaR-nh <sub>2</sub>							
<b>Sarcotoxins</b>								
S.p. Ia	gWlkKigK <b>Kk</b> IERvGQhtRDATIqAlgiagqaAnvaataRg-nh <sub>2</sub>							
S.p. Ib	gWlkKigK <b>Kk</b> IERvGQhtRDATIqvgivagqaAnvaataR-nh <sub>2</sub>							
S.p. Ic	gWlrKigK <b>Kk</b> IERvGQhtRDATIqvlgiagqaAnvaataR-nh <sub>2</sub>							

FIGURE 1 Sequence alignment of cecropin A, B, and D (from *Hyalophora cecropia*, *Bombyx mori*, and *Antheraea pernyi*) with bactericidins (from *Manduca sexta*) and sarcotoxins (from *Sarcophaga peregrina*). Residues identical among the cecropins and that also occur in the other sequences are indicated as bold capital letters. Single conservative substitutions among the cecropins and that also occur in the other sequences are indicated as regular capital letters. The PAM120 mutation matrix was used to judge conservative substitutions (33).

quences (Lys 6, Glu 9, Gly 12, and Arg 16). There are an additional seven residues that are identical among the cecropins (Trp 2, Phe 5, Ala 22, Gly 23, Pro 24, Ala 25, and Ala 32). The Ala 22-Gly 23-Pro 24-Ala 25 hinge sequence (described above) is among the latter group. Although the hinge is not strictly conserved among the superfamily, the other peptides have helix breaking glycine and/or proline residues at this location. Considering the overall similarity, it is likely that the bactericidin and sarcotoxin peptides adopt similar structures to the cecropins and act to lyse bacterial cell membranes in an analogous manner.

Fig. 2 shows the pattern of conserved residues around the NH<sub>2</sub>-terminal helix of cecropin A. The feature of unilateral conservation is seen, where the identical residues among the cecropin sequences are clustered along one face of the helix. The sites of single conservative substitutions radiate from the identical residues around both sides of the helix. Fig. 2 also shows the sharp partitioning of hydrophilic and hydrophobic residues around the NH<sub>2</sub>-terminal helix (previously described by Steiner [13] and Merrifield et al. [14]). This amphipathic pattern is a commonly observed feature of membrane bound peptides. The COOH-terminal helix is less amphipathic with the hydrophobic surface being at least twice as large as the hydrophilic surface (not shown).

### Dimer model

It is generally observed that conserved residues play important roles in protein structure and function and are often involved in interprotein contacts in oligomeric structures (24, 25). Based on this principle, an antiparallel dimer model was constructed to place the highly conserved NH<sub>2</sub>-terminal helix residues (those conserved among the superfamily) in contact with each other. (It is

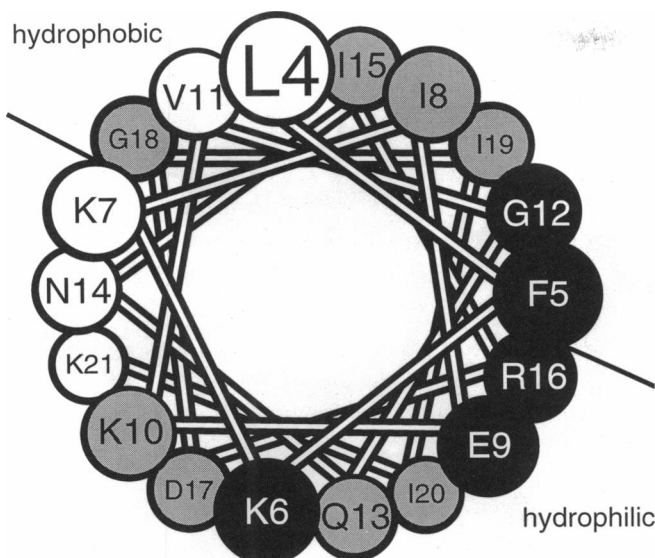


FIGURE 2 Helical wheel projection of the NH<sub>2</sub>-terminal sequence (residues 4–21) of cecropin A. The residues identical within the cecropins (Fig. 1) are shaded dark gray, and the residues at locations of conservative single substitutions are shaded light gray.

unlikely that the conserved residues in cecropin are involved in binding to a membrane bound receptor or other protein, because the all-D amino acid enantiomer of cecropin A was found to have the same antibacterial activity as the native, all-L form [26].) Fig. 3 *a* shows the dimer in a schematic of the bilayer membrane (this is similar to the initial bound states proposed by Christensen et al. [7] and Fink et al. [16]). The NH<sub>2</sub>-terminal helices are sunken into the head-group layer of the membrane, and the COOH-terminal helices span the aliphatic phase of the membrane. Fig. 3 *b* displays a top view of the NH<sub>2</sub>-terminal helices coded for sequence conservation. The dimer configuration allows for two salt-bridges to be formed between the conserved Glu 9 and Arg 16 residues of opposite cecropin strands. The conserved Phe 5 residues rest on top of the conserved Pro 24 residues of the adjacent peptides. The NH<sub>2</sub>-terminal helices were found to pack best in the cross-ridge motif with a crossing angle of  $-20^\circ$  (27) (in contrast to the knobs-into-holes [28] and ridges-into-grooves [27] motifs). The close packing of the helices is facilitated by the small, conserved Gly 12 residues near the intersection.

Fig. 4 *a* shows the pattern of hydrophilic and hydrophobic residues on the dimer surface. When bound to the membrane, the hydrophilic residues of the NH<sub>2</sub>-terminal helices are in contact with the polar head-groups of the lipid molecules on the sides and with the solvent molecules on the top. The hydrophobic residues on the bottom of the NH<sub>2</sub>-terminal helices are in contact with the lipid alkyl chains. Fig. 4, *b* and *c* show explicit conformations for how phosphatidylethanolamine molecules may bind to the dimer. The lipid molecules of the bottom half of the membrane bilayer are assumed to be

in the regular, perpendicular orientation and are not shown. Because the NH<sub>2</sub>-terminal helices are sunken into the top head-group layer of the membrane, the alkyl chains of the lipid molecules fold underneath the dimer. This has the result of thinning the top lipid monolayer of the membrane. The thinning of the top monolayer allows the 25 Å long COOH-terminal helices to completely span the alkyl phase of the membrane, which is normally  $\sim 30$  Å thick.

### Type I channel

The simplest type of channel structure we envisioned is shown in Fig. 5, in which six of the membrane bound dimers are arranged in a circular pattern like the spokes of a wheel. The pore is formed by the six adjacent COOH-terminal helices, with the polar faces oriented toward the center. Fig. 5 *b* shows a detailed top view of the pore structure. The narrowest part of the pore is formed by the six Gln 31 and Gln 34 residues, which form two stacked, hydrogen bonded rings (see also Fig. 3 *a*). A similar single ring structure occurs in models of the alamethicin channel, in which the Gln 7 residues are postulated to regulate the pore size and conductance (29). It should be noted that alamethicin has a weak

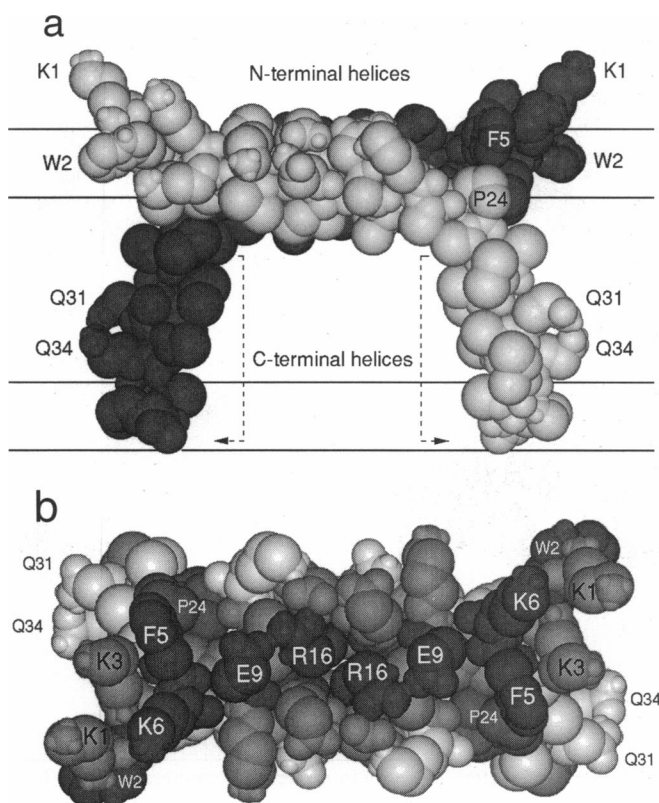
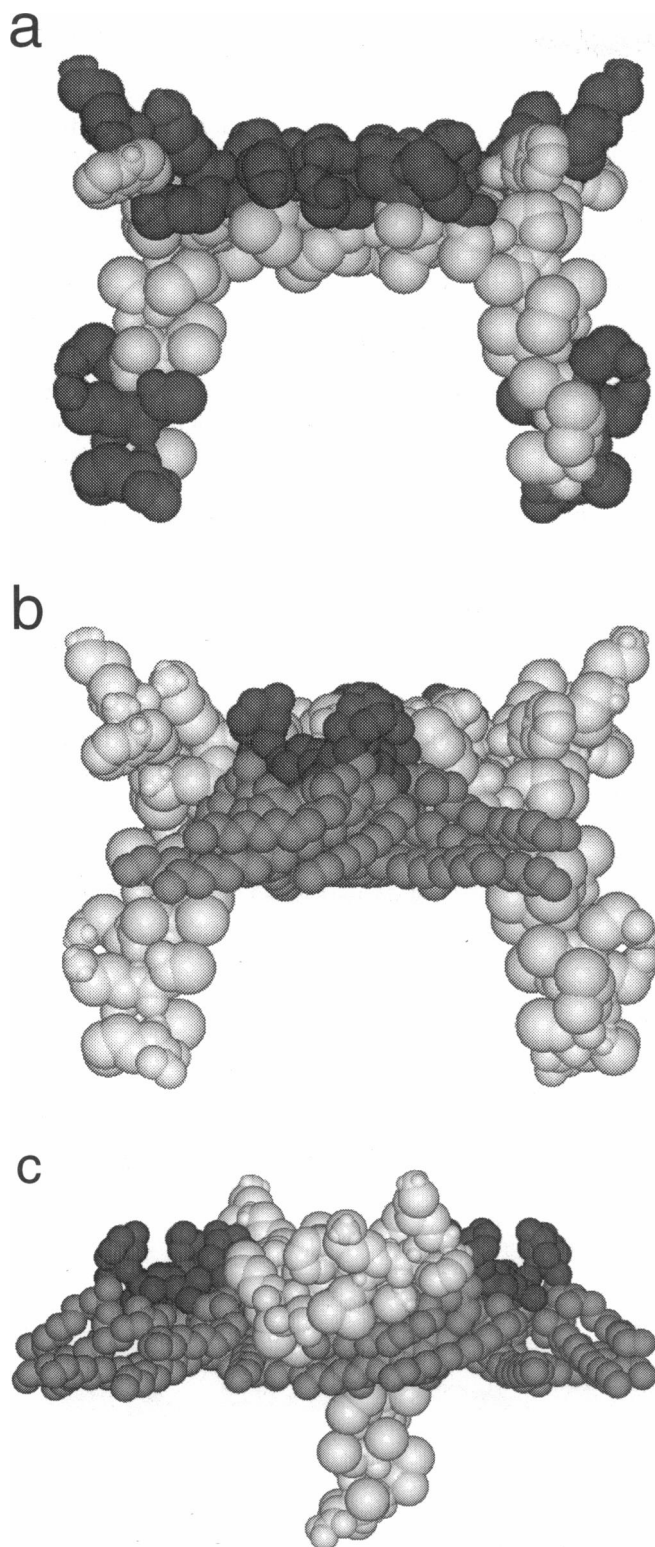
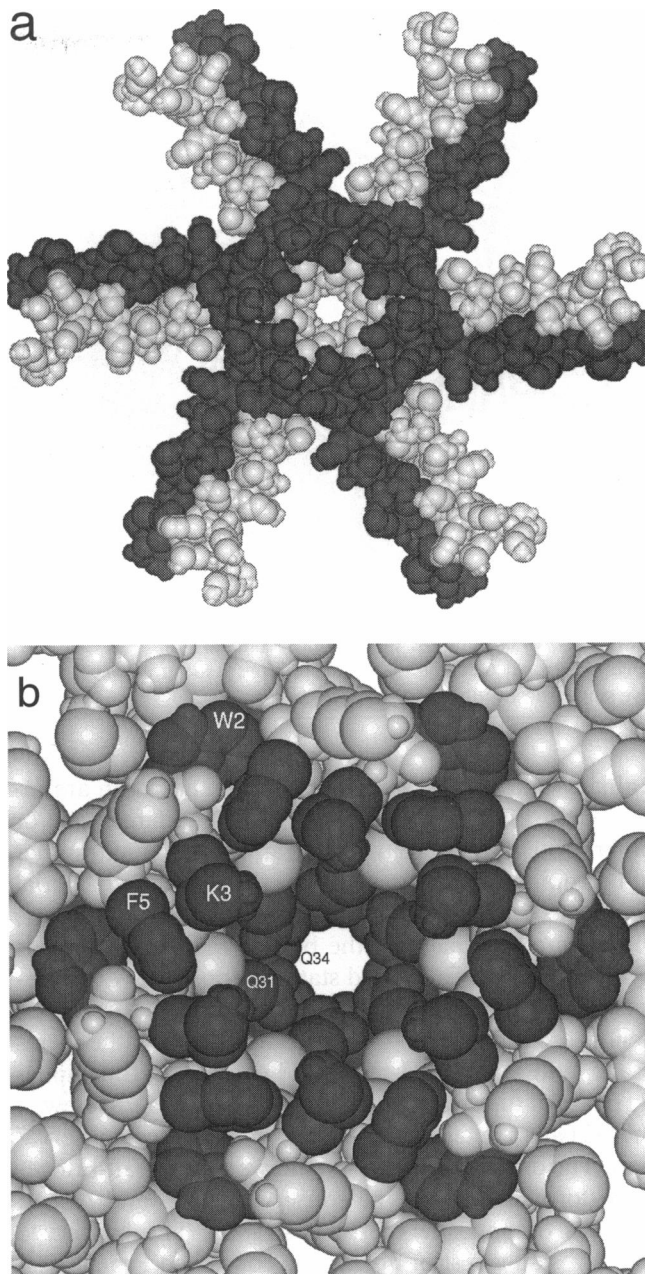


FIGURE 3 Antiparallel dimer of cecropin A. (*a*) Position of the dimer in membrane bilayer. (*b*) Top view coded for sequence conservation. The residues identical within the cecropin sequences are shaded dark gray, and the residues at locations of conservative single substitutions are shaded light gray.



**FIGURE 4** Interaction of cecropin dimer with membrane lipids. (a) Distribution of hydrophilic and hydrophobic residues on the dimer. The hydrophilic residues are shaded gray. (b) Side view of phosphatidylethanolamine lipid molecules bound to dimer. The bottom monolayer of the membrane lipids is not shown. The lipid head-groups are shaded dark gray, and the alkyl chains are shaded light gray. (c) End-on view of membrane bound dimer. The front COOH-terminal helix was removed to expose the underlying alkyl chains.



**FIGURE 5** Top view of the type I channel model of cecropin A. (a) One peptide in each of the dimers is shaded. (b) Detailed view of the pore structure. The Trp 2, Lys 3, Phe 5, Gln 31, and Gln 34 residues are labeled. The Lys 1 and Asp 9 sidechains were removed to expose the Trp 2 and Phe 5 residues. The Ile 8 residues are beneath the Trp 2 residues.

cation selectivity, whereas the chimeric cecropin AD has a weak anion selectivity ( $\text{Cl}^-/\text{Na}^+ = 2:1$ ) (7). However, the anion selectivity in cecropin may be due to the rings of positively charged Lys 1, Lys 3, and Lys 37 residues around the pore entrances. Glutamine residues also have been postulated to play a role in the gating mechanism of the [Leu<sup>1</sup>]zervamicin channel (30). In the type I model of cecropin A, the inner diameter of the glutamine rings is 5.6 Å, which is large enough to allow the passage of

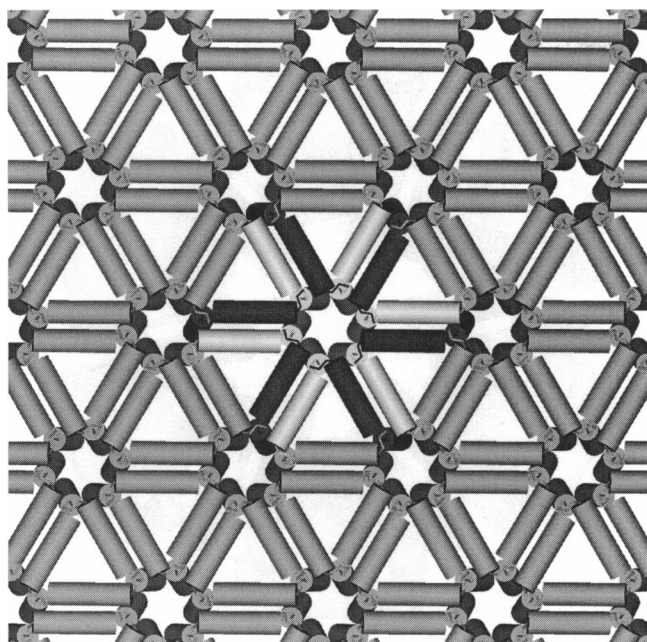


FIGURE 6 Top view of hexagonal lattice structure of cecropin A. The  $\text{NH}_2$ - and  $\text{COOH}$ -terminal helices of the peptides are displayed as cylinders for clarity. A complete type I channel is highlighted in dark and light grey. The  $\text{COOH}$ -terminal helices form the pores at the sites of sixfold symmetry.

solvated  $\text{Na}^+$  and  $\text{Cl}^-$  ions. This is similar to the frog muscle endplate acetylcholine-activated receptor channel, which has an experimentally determined minimum diameter of  $6.4 \text{ \AA}$  (31). It should be pointed out, however, that we cannot predict the exact number of dimers that will be involved in forming the type I pores. However, pores of type I channel models built with less than four dimers (not shown) appear too small to conduct ions.

As seen in Fig. 5 *b*, the conserved Trp 2 residue from one dimer fits into a hydrophobic pocket formed from the conserved Phe 5 and Ile 8 residues (Leu 8 in cecropin D) of the adjacent dimer (located clockwise looking from the top: the Ile 8 residue is directly underneath the Trp 2 residue). This packing occurs in six symmetric locations around the mouth of the pore. The formation of these hydrophobic interactions serve to stabilize the channel structure. This would explain why the substitution of Trp 2 to first a phenylalanine and then a glutamate residue leads to a progressive reduction in antibacterial activity (18).

As shown in Fig. 6, the sixfold symmetry of the type I model naturally lends itself to the formation of a hexagonal lattice, in which each monomer has identical interactions with the surrounding molecules. In this structure, a transmembrane pore is formed at each site of sixfold symmetry by six  $\text{COOH}$ -terminal helices. The lipid head-groups (not shown) would be sequestered in the triangular regions between the  $\text{NH}_2$ -terminal helices.

The thinning of the top layer of the membrane described for the bound dimer (see above) would be extended over the range of the lattice. The membrane surface area per peptide in the type I lattice is  $453 \text{ \AA}^2/\text{peptide}$ , which corresponds to the areas calculated for the LD50 concentrations of cecropin A with *E. coli* and *B. megaterium* ( $660$  and  $400 \text{ \AA}^2/\text{peptide}$ ) (6).

## Type II channels

The second class of channel models (type II) have the pore formed from the  $\text{NH}_2$ -terminal helices rather than from the  $\text{COOH}$ -terminal helices. Channels of this type have been proposed by Christensen et al. (7) and Fink et al. (16). An important consideration in forming the type II models is that the  $\text{NH}_2$ -terminal helices are highly charged (e.g., cecropin A has 8 positive and 2 negative formal charges). It is unlikely that the  $\text{NH}_2$ -terminal helices would insert individually into the hydrophobic phase of the membrane and then form the channel, because this would require a considerable amount of energy to remove the bound water molecules and lipid head-groups from the charged residues. Instead, Fig. 7 diagrams a concerted conformational change by which the hydrophilic residues of the  $\text{NH}_2$ -terminal helices can move from the membrane surface to the pore lining without encountering the hydrophobic phase of the membrane. The relative orientations of the two  $\text{NH}_2$ -terminal helices in the dimers, and thus the contacts between the conserved residues (see Fig. 3 *b*), are maintained between the type I to type II models. Fig. 7 *a*

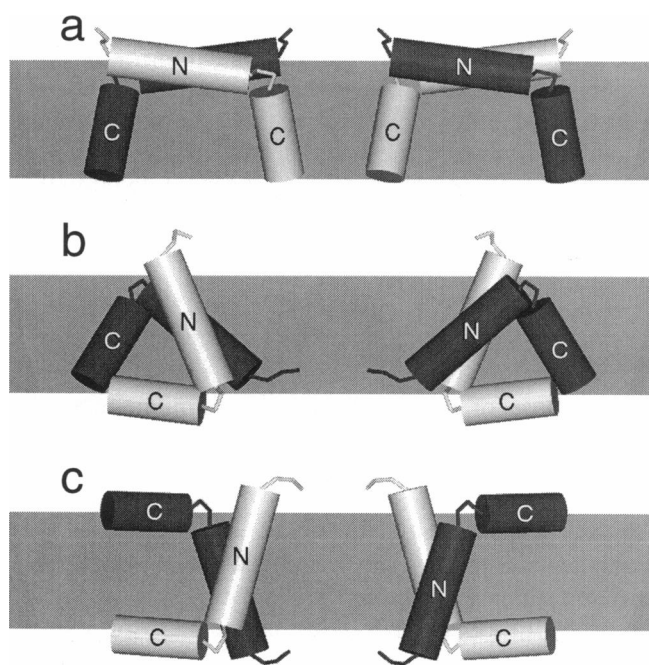


FIGURE 7 Conformational change from the type I to type II channel structures. Cross-sections through the (a) type I, (b) type IIa, and (c) type IIb models.



shows a cross-section of the type I channel in Fig. 5. Fig. 7 *b* illustrates the type IIa channel, in which the central COOH-terminal helices have moved to the opposite side of the membrane and the NH<sub>2</sub>-terminal helices are at a 45° angle to the membrane plane. Fig. 7 *c* illustrates the type IIb channel, in which the outer COOH-terminal helices have moved to the top membrane surface and the NH<sub>2</sub>-terminal helices are perpendicular to the membrane plane. The NH<sub>2</sub>-terminal helices are 35 Å long, which enables them to completely span the membrane core.

The type IIa and IIb channels are shown in Fig. 8 (the peptides are displayed as cylinders for clarity). In the figures, the channels are surrounded by six dimers in the type I orientation, which shows how both type I and II channels can be incorporated in the lattice structure of Fig. 6. The net positive charge of the NH<sub>2</sub>-terminal helices, which form the pores of the type II channels, would likely cause the observed anion selectivity (7). Unlike the type I and type IIa models, the structure of the type IIb channel is symmetric with respect to both sides of the membrane. This would likely cause a symmetric current-voltage curve similar to that observed for the cecropin AD peptide (7). The pore size of the type II models is larger than the type I model (11 and 15 Å for the narrowest regions of the type IIa and IIb channels versus 5.6 Å for the type I channel). The fact that the cecropin AD peptide displays two distinct conductance states (0.4 and 1.93 nS) (7) suggests that both the type I and II channel structures are possible for this chimeric peptide.

Fig. 8 *b* shows a cross-section of the type IIa channel. This demonstrates how the lipid head-groups, which are bound to the sides of the NH<sub>2</sub>-terminal helices in the type I model, could be brought into the lining of the type II pores. In going to the type IIb channel, the head-groups could either move back to the membrane surface or remain bound to the sides of the NH<sub>2</sub>-terminal helices. The possibility of lipids being incorporated into the pores of peptide channels deserves some attention, as the size and charges of the head-groups may influence the ion gating and selectivity.

## DISCUSSION

The purpose of this work was to assimilate what is known and inferred about the structure and function of cecropin into three-dimensional computer models, which can then be used to design further experiments. The use of an atomic-scale versus a more generalized model enables the investigator to determine what structures are sterically possible. In evaluating this work it is important to assess the validity of the basic principles and assumptions, the uniqueness of the resulting models, how they compare with previous models, and what insights and experiments they suggest.

The first assumption was that each peptide has the helix-bend-helix secondary structure motif predicted by

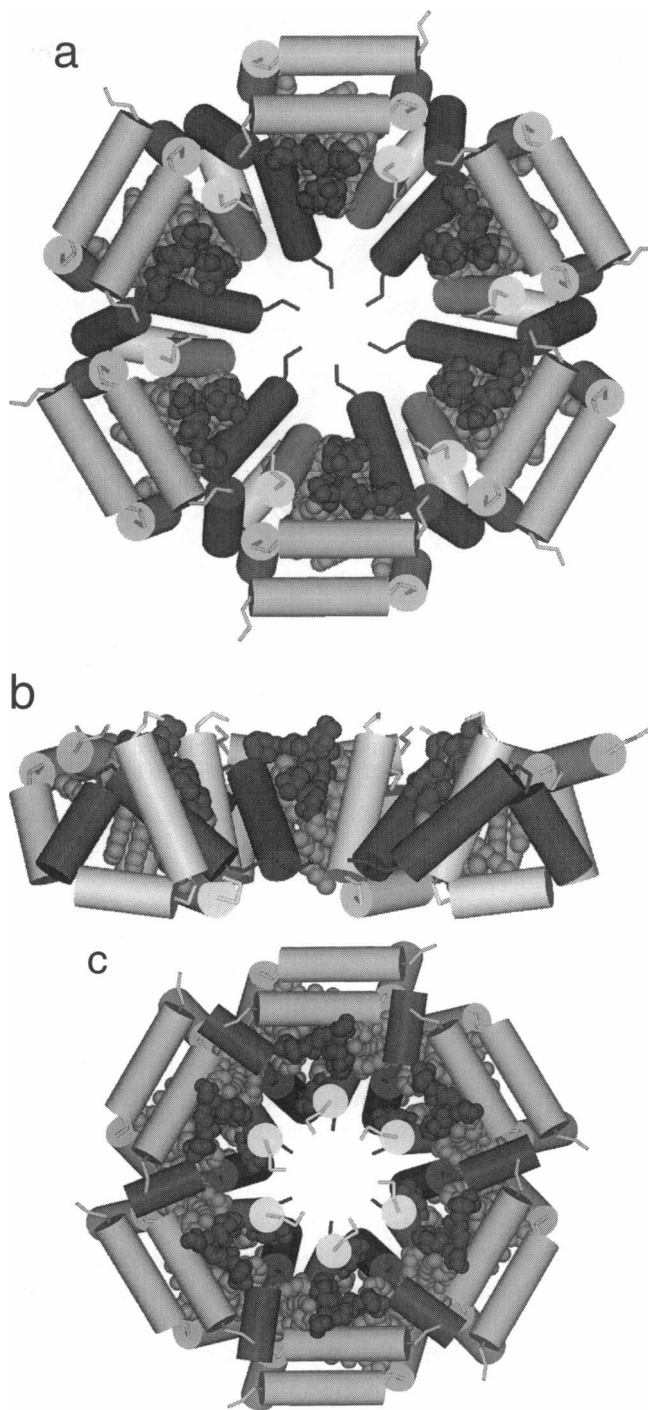


FIGURE 8 Type II channel models. The NH<sub>2</sub>- and COOH-terminal helices are shown as cylinders for clarity. The lipid head-groups are shaded dark gray, and the alkyl chains are shaded light gray. (a) Top view of the type IIa channel. (b) Side view cut-away of the type IIa channel. (c) Top view of type IIb channel.

sequence analysis and circular dichroism spectroscopy (13, 14) and determined by NMR in reduced polarity solvent (15).

The next step was to use the sequence and secondary structure information to predict how cecropin peptides

would bind to the membrane and combine with each other. Because of the amphipathic character (Fig. 2), the NH<sub>2</sub>-terminal helices are expected to lie parallel in the hydrophilic head-group/hydrophobic alkyl-chain interface of the membrane. This satisfies the thermodynamic constraint that the hydrophilic residues are in contact with the polar head-groups and/or water and the hydrophobic residues are in contact with the alkyl-chains (7, 16).

The pattern of amino acid conservation was then used to predict the most plausible interaction between cecropin peptides. The main assumption was that the conserved residues play important roles in the structure and/or function of the protein (25, 26). As seen in Fig. 2, the zone of conserved residues in the NH<sub>2</sub>-terminal helix of cecropin A straddles one of the interfaces between the hydrophobic and hydrophilic residues. This is in contrast to most amphipathic helices in soluble proteins, for which primarily the hydrophobic face is conserved, and for most transmembrane helices in integral membrane proteins, for which primarily the hydrophilic face is conserved. If the linear-helix structure is accepted for the NH<sub>2</sub>-terminal region of cecropin, then it is impossible for the conserved residues to be involved in contacts within a single peptide. Likewise, the finding that the all L- and D-amino acid forms of cecropin have similar activity (26) indicates that the conserved residues are also not involved in binding to a hitherto unknown membrane protein and/or receptor. Thus, the conserved residues are likely involved in binding multiple peptides together. Given the orientation of the NH<sub>2</sub>-terminal helices parallel to the membrane, and the spread of the conserved residues along only one of the hydrophobic/hydrophilic interfaces, the only way to bring the conserved helix surfaces together is to form an antiparallel dimer (see Fig. 3). As described in Methods and Results, the specific interhelical orientation and residue contacts were dictated by optimization of the packing. Thus, it is seen how basic assumptions, theoretical principles, and experimental data are combined to form a unique model for cecropin aggregation in the membrane.

A number of experiments could be done to test whether antiparallel dimers form between membrane-bound cecropin peptides. For example, the model in Fig. 3 can be used to predict where cysteine residues could be substituted into the sequence to form detectable disulfide bridges between the NH<sub>2</sub>-terminal helices. Likewise, fluorescent probes could be added to measure distances by energy transfer. As also described in Fig. 3, salt-bridges are predicted to form between the conserved Glu 9 and Arg 16 residues. The substitution of either of these residues to one of opposite or neutral charge should reduce the binding of the peptides and thus reduce the activity. In contrast, simultaneously mutating Glu 9 to arginine and Arg 16 to glutamate might maintain the peptide binding affinities and measured activity.

The antiparallel dimer model is a unique structure developed from the principles and procedures outlined above. However, the prediction of the channel structure is less well defined. The first assumption was that the channels are built from a collection of the dimer subunits. This is reasonable if the dimer is accepted to be a stable, low energy structure. Given that the channels are constructed of identical subunits, it is reasonable to assume that the channels have a rotational axis of symmetry down the center of the pore. These two assumptions drastically reduce the number of different channel structures that can be imagined. Unfortunately, the number of cecropin peptides that actually form a channel structure is not experimentally known. This information would also help to limit the number of possible models. We have chosen to illustrate the type I and type II channel models with six dimers, because this produces reasonable pore dimensions and forms a simple hexagonal lattice. Four dimers are predicted to be the lower limit, because type I channel structures built with less than four dimers appear not to have pores large enough to conduct ions.

It is also unknown whether the pore of the channel is formed by the NH<sub>2</sub>- or COOH-terminal helices. Christensen et al. (7) and Fink et al. (16) have proposed that the pore is formed by the positively charged NH<sub>2</sub>-terminal helices, due to the requirement of a positive potential on the same side of the membrane as the added peptides for conductance. However, the COOH-terminal helices also have a positive charge at the end, due to a lysine residue and COOH-terminal amidation (see Fig. 1), and the positive potential requirement could also reflect the insertion and/or alignment of these helices into the hydrophobic phase of the membrane. In either case, Fig. 7 demonstrates how the NH<sub>2</sub>-terminal helices could be inserted into the membrane core and form a pore without having to desolvate the charged residues. It should be noted, however, that the observation of two distinct conduction states for the cecropin AD peptide (7) supports the hypothesis that both the type I and II channels, which have different sized pores, are physiologically active.

The type I and II channel models can be used to suggest experiments to determine whether the active pores are formed by the NH<sub>2</sub>- or COOH-terminal helices or whether both types of channels exist. For example, in the type I model of cecropin A (Fig. 5) the narrowest region of the pore is formed by two hydrogen bonded rings of the Gln 31 and Gln 34 residues. If this type of pore does exist, then the substitution of the glutamines to residues of different size and/or charge should affect the current and/or selectivity. Likewise, mutations of the hydrophilic residues of the NH<sub>2</sub>-terminal helices should affect the conductance properties if the type II model pore is active. It was also described how lipid head-groups could be incorporated into the lining of the type II pore (Fig. 8). If this does occur, then changes in the charge and/or

size of the head-groups should also affect the conduction properties of the type II pore.

An interesting question about the activity of cecropin (and magainin as well) is why such a large number of peptides are required to be bound to the bacterium to be lethal. Steiner et al. (6) estimated that the quantity of bound cecropin molecules is sufficient to form a monolayer over the membrane surface. This is in contrast to the protein colicin (32), for which only one bound molecule may be lethal. Citing the similar concentration and sequence dependencies for channel formation and antibacterial activity, Christensen et al. (7) concluded that the main lethal effect of cecropin is the formation of ion channels in the bacterial membrane. Although not ruling out the initial formation of pores, the high density of bound peptides led Steiner et al. (6) to suggest that the main lethal effect is the disintegration of the membrane. It would seem that if Christensen et al. (7) is right, then the channels would be formed only when the peptide density on the membrane is high. This is because even a few large channels formed at low peptide density would likely be lethal.

We formulated the channel models as part of a lattice (Fig. 6) to accommodate the calculated high packing density of the peptides on the membrane surface (6). It must be noted that there is no experimental evidence for a regularized lattice structure. However, the formation of at least a partial lattice would not be unexpected, as this would be an evenly distributed, low energy structure. The hexagonal geometry was chosen for illustration purposes because it provides reasonable pore dimensions for cecropin A and AD (5.6 and 15 Å) based on their conductances (7) and in comparison with other channels. However, a smaller square lattice geometry may be appropriate for the cecropin B and D peptides, which have lower single channel conductances than cecropin A (0.035, 0.026, and 0.007 versus 0.16 nS) (7). It was described how the binding of the peptides leads to thinning of the top lipid monolayer of the membrane over the extent of the lattice. This phenomenon could facilitate the membrane disintegration proposed by Steiner et al. (6). It would be of considerable interest to attempt to grow two-dimensional crystals of cecropin and measure the unit-cell dimensions. If the lattice does exist, then this information would provide useful constraints for model development.

It is important to consider that the formation of an extended type I lattice, in which the NH<sub>2</sub>-terminal helices of cecropin are sunken in between the headgroups, would cause an expansion of the outer lipid monolayer of the bacterial cell membrane. Since the outer and inner membrane monolayers are geometrically constrained to have approximately the same surface area, the expansion pressure may drive the formation of the type II channels, which affect both sides of the bilayer equally. This mechanism could explain why many cecropin peptides must bind to the cell to be lethal and agrees with the postulate

of Christensen et al. (7) and Fink et al. (16) that the NH<sub>2</sub>-terminal helices must be inserted into the membrane to cause cell death. It should be noted that the expansion-pressure mechanism would not occur in the planar bilayer system in vitro, in which the *cis* and *trans* monolayers can expand independently. This could explain the positive voltage requirement for conductance observed by Christensen et al. (7) for the in vitro system.

The models presented here for the cecropin channels are the best we could develop that satisfy the experimental data and physiochemical principles (see Methods). Unfortunately, there does not currently exist a comprehensive method to systematically search and determine the most probable channel structures. Ideally, the likelihoods of proposed models would be ranked by their relative free energies. However, it is presently beyond the scope of computer simulations to calculate free energy differences for systems of this size, which must include both enthalpic and entropic contributions to the interactions between the peptides, lipids, water, ions, and membrane voltage. This being the case, we would like to stress that even if the overall peptide configurations are correct, then the models should only be considered as approximations of the actual atomic structure. This is especially true for the lipid molecules, which were used to determine possible modes of peptide binding to the membrane. In reality, the lipids are expected to undergo large and continuous conformational changes. Despite these shortcomings, the channel models serve as descriptive examples of different classes of assemblies and provide working hypotheses for future experiments.

## REFERENCES

1. Steiner, H., D. Hultmark, A. Engström, H. Bennich, and H. G. Boman. 1981. Sequence and specificity of two antibacterial proteins involved in insect immunity. *Nature (Lond.)* 292:246-248.
2. Hultmark, D., H. Steiner, T. Rasmuson, and H. G. Boman. 1980. Insect immunity. Purification and properties of three inducible bactericidal protein from hemolymph of immunized pupae of *Hyalophora cecropia*. *Eur. J. Biochem.* 106:7-16.
3. Hultmark, D., A. Engström, H. Bennich, R. Kapur, and H. G. Boman. 1982. Insect immunity: isolation and structure of cecropin d and four minor antibacterial components from cecropia pupae. *Eur. J. Biochem.* 127:207-217.
4. Qu, X.-M., H. Steiner, A. Engström, H. Bennich, and H. G. Boman. 1982. Insect immunity: isolation and structure of cecropins B and D from pupae of the chinese oak silk moth, *Anthea pernyi*. *Eur. J. Biochem.* 127:219-224.
5. Teshima, T., Y. Ueki, T. Nakai, and T. Shiba. 1986. Structure determination of lepidopteran, self-defense substance produced by silkworm. *Tetrahedron* 42:829-834.
6. Steiner, H., D. Andreu, and R. B. Merrifield. 1988. Binding and action of cecropin analogues: antibacterial peptides from insects. *Biochim. Biophys. Acta* 939:260-266.
7. Christensen B., J. Fink, R. B. Merrifield, and D. Mauzerall. 1988. Channel-forming properties of cecropins and related model compounds incorporated into planar lipid membranes. *Proc. Natl. Acad. Sci. USA* 85:5072-5076.



8. Hall, J. E., I. Vodyanoy, T. M. Balasubramanian, and G. R. Marshall. 1984. ALAMETHICIN: a rich model for channel behavior. *Biophys. J.* 45:233–247.
9. Duclohier, H., G. Molle, and G. Spach. 1989. Antimicrobial peptide magainin I from *Xenopus* skin forms anion-permeable channels in planar lipid bilayers. *Biophys. J.* 56:1017–1021.
10. Mellor, I. R., D. H. Thomas, and M. S. P. Sansom. 1988. Properties of ion channels formed by *Staphylococcus aureus*  $\delta$ -toxin. *Biochim. Biophys. Acta.* 942:280–294.
11. Kagan, B. L., M. E. Selsted, T. Ganz, and R. I. Lehrer. 1990. Antimicrobial defensin peptides form voltage-dependent ion-permeable channels in planar lipid bilayer membranes. *Proc. Natl. Acad. Sci. USA* 87:210–214.
12. Lazarovici, P., N. Primor, and L. M. Loew. 1986. Purification and pore-forming activity of two hydrophobic polypeptides from the secretion of the red sea moose sole (*Pardachirus marmoratus*). *J. Biol. Chem.* 261:16704–16713.
13. Steiner, H. 1982. Secondary structure of the cecropins: antibacterial peptides from the moth *Hyalophora cecropia*. *FEBS (Fed. Eur. Biochem. Soc.) Lett.* 137:283–287.
14. Merrifield, R. B., L. D. Vizioli, and H. G. Boman. 1982. Synthesis of the antibacterial peptide cecropin A(1–33). *Biochemistry.* 21:5020–5031.
15. Holak, T. A., A. Engström, P. J. Kraulis, G. Lindeberg, H. Bennich, T. A. Jones, A. M. Gronenborn, and G. M. Clore. 1988. The solution conformation of the antibacterial peptide cecropin A: a nuclear magnetic resonance and dynamical simulated annealing study. *Biochemistry.* 27:7620–7629.
16. Fink, J., A. Boman, H. G. Boman, and R. B. Merrifield. 1989. Design, synthesis and antibacterial activity of cecropin-like model peptides. *Int. J. Pept. Protein Res.* 33:412–421.
17. Boman, H. G., I. Faye, P. V. Hofsten, K. Kockum, J.-Y. Lee, K. G. Xanthopoulos, H. Bennich, A. Engström, R. B. Merrifield, and D. Andreu. 1985. On the primary structures of lysozyme, cecropins and attacins from *Hyalophora cecropia*. *Dev. Comp. Immunol.* 9:551–558.
18. Andreu, D., R. B. Merrifield, H. Steiner, and H. G. Boman. 1985. N-terminal analogues of cecropin A: synthesis, antibacterial activity, and conformational properties. *Biochemistry.* 24:1683–1688.
19. Fink, J., R. B. Merrifield, A. Boman, and H. G. Boman. 1989. The chemical synthesis of cecropin D and an analog with enhanced antibacterial activity. *J. Biol. Chem.* 264:6260–6267.
20. Richardson, J. S., and D. C. Richardson. 1988. Amino acid preferences for specific locations at the ends of  $\alpha$ -helices. *Science (Wash. DC).* 240:1648–1652.
21. Brooks, B. R., R. E. Bruccoleri, B. D. Olafson, D. J. States, S. Swaminathan, and M. Karplus. 1983. CHARMM: a program for macromolecular energy, minimization, and dynamics calculations. *J. Comp. Chem.* 4:187–217.
22. Dickinson, L., V. Russell, and P. E. Dunn. 1988. A family of bacteria-regulated, cecropin D-like peptides from *Manduca sexta*. *J. Biol. Chem.* 263:19424–19429.
23. Okada, M., and S. Natori. 1985. Primary structure of sarcotoxin I, an antibacterial protein induced in the hemolymph of *Sarcophaga peregrina* (flesh fly) larvae. *J. Biol. Chem.* 260:7174–7177.
24. Go, M., and S. Miyazawa. 1980. Relationship between mutability, polarity and exteriority of amino acid residues in protein evolution. *Int. J. Pept. Protein Res.* 15:211–224.
25. Sander, C., and R. Schneider. 1991. Database of homology-derived protein structures and the structural meaning of sequence alignment. *Proteins* 9:56–68.
26. Wade, D., A. Boman, B. Wählin, C. M. Drain, D. Andreu, H. G. Boman, and R. B. Merrifield. 1990. All-D amino acid-containing channel-forming antibiotic peptides. *Proc. Natl. Acad. Sci. USA.* 87:4761–4765.
27. Chothia, C., M. Levitt, and D. Richardson. 1981. Helix to helix packing in proteins. *J. Mol. Biol.* 145:215–250.
28. Crick, F. H. C. 1953. The packing of  $\alpha$ -helices: simple coiled-coils. *Acta Crystallogr.* 6:689–697.
29. Fox, R. O., and F. M. Richards. 1982. A voltage-gated ion channel model inferred from the crystal structure of alamethicin at 1.5-Å resolution. *Nature (Lond.)* 300:325–330.
30. Karle, I. L., J. L. Flippen-Anderson, S. Agarwalla, and P. Balaram. 1991. Crystal structure of [Leu<sup>1</sup>]zervamicin, a membrane ion-channel peptide: implications for gating mechanisms. *Proc. Natl. Acad. Sci. USA.* 88:5307–5311.
31. Dwyer, T. M., D. J. Adams, and B. Hille. 1980. The permeability of the endplate channel to organic cations in frog muscle. *J. Gen. Physiol.* 75:469–492.
32. Cramer, W. A., F. S. Cohen, A. R. Merrill, and H. Y. Song. 1990. Structure and dynamics of the colicin E1 channel. *Mol. Microbiol.* 4:519–526.
33. Dayhoff, M. O., R. M. Schwartz, and B. C. Orcutt. 1978. A model of evolutionary change in proteins. In *Atlas of Protein Sequence and Structure*. Vol. 5. Suppl. 3. M. O. Dayhoff, editor. National Biomedical Research Foundation, Washington, DC. 345–352.